

Large-mass ultralow noise germanium detectors: performance and applications in neutrino and astroparticle physics

P S Barbeau¹, J I Collar¹ and O Tench²

¹ Department of Physics, Enrico Fermi Institute and Kavli Institute for Cosmological Physics, University of Chicago, Chicago, IL 60637, USA

² CANBERRA Industries, 800 Research Parkway, Meriden, CT 06450, USA

E-mail: collar@uchicago.edu

Received 26 April 2007

Accepted 8 August 2007

Published 11 September 2007

Online at stacks.iop.org/JCAP/2007/i=09/a=009

doi:10.1088/1475-7516/2007/09/009

Abstract. A new type of radiation detector, a p-type modified electrode germanium diode, is presented. It is shown that the prototype displays, for the first time, a combination of features (mass, energy threshold and background expectation) required for a measurement of coherent neutrino–nucleus scattering in a nuclear reactor experiment. First results are presented from its calibration using sub-kiloelectronvolt nuclear recoils similar to those expected from reactor antineutrinos or light WIMPs (weakly interacting massive particles) beyond the reach of present detectors. The device hybridizes the mass and energy resolution of a conventional HPGe coaxial gamma spectrometer with the low electronic noise and threshold of a small x-ray semiconductor detector, also displaying an intrinsic ability to distinguish multiple-site from single-site particle interactions. The present performance of the prototype and possible further improvements are discussed, as well as other applications for this new type of device in neutrino and astroparticle physics (double-beta decay, neutrino magnetic moment and novel WIMP searches).

Keywords: dark matter detectors, neutrino experiments, neutrino detectors, neutrino properties

JCAP09(2007)009

Contents

1. Introduction	2
2. A first coherent neutrino detector	3
3. Applications beyond coherent neutrino scattering	11
4. Conclusions	17
Acknowledgments	17
References	17

1. Introduction

From an experimental point of view, the detection of the soft nuclear recoils expected from coherent scattering of low energy neutrinos off nuclei [1, 2] remains a daunting challenge. The applications of a capable detector to fundamental and applied physics would be numerous: a large coherent enhancement to the cross-section for this process results in expected recoil rates in the hundreds per kilogram of target per day from reactor antineutrinos, affording a radical detector compaction. Of all artificial neutrino sources, power reactors offer by far the largest flux, with essentially all (anti)neutrino energies being able to interact coherently. The difficulty resides in a majority of these recoils falling well below the energy threshold of conventional detector technologies. Until now, no device has met the minimum target mass (>1 kg) and energy threshold ($E_{\text{rec}} < 1$ keV) required for such a measurement, with the possible exception of [3]³. Unrealized proposals nevertheless abound [2, 4, 5]. Not only the recoil energies themselves are low, but only a fraction of these are generally available in a readily detectable form (ionization, scintillation). A characterization of this fraction (the ‘quenching factor’) and a precise definition of signal acceptance near the detector threshold are necessary first steps in the development of a coherent neutrino detector. In a companion paper [6], an approach to this challenging in itself calibration exercise has been developed.

The advent of a coherent neutrino detection technology would enable true technological applications [7], for instance, non-intrusive monitoring of nuclear reactors against illegitimate uses (e.g., fuel rod diversion, production of weapons-grade material) with a truly compact device, improving on proposed methods [8] that rely on standard (charged current) ton-sized neutrino detectors. Beyond these, the interest in observing this process is not merely academic: a neutral-current detector responds essentially the same way to all known neutrino types [9]. Therefore, the observation of neutrino oscillations in such a device would constitute as close to *direct* evidence for sterile neutrino(s) as is possible. Separately, the cross-section for this process is critically dependent on a neutrino magnetic moment: disagreement with the standard model prediction can reveal

³ Low recoil energy thresholds have been achieved in sapphire bolometers before [3]. Using the same threshold definition and experimental reactor conditions considered for the detector described here, the recoil rate above their effective threshold of ~ 1.5 keV would be ~ 3.5 antineutrino-induced recoils $\text{kg}^{-1} \text{day}^{-1}$.

a finite value presently beyond reach [10]. Recently the strong sensitivity of the process to non-standard neutrino interactions with quarks [11] and the effective neutrino charge radius [12] has been emphasized. Other fundamental physics applications can be listed: a precise enough measurement of the cross-section would constitute a sensitive probe of the weak nuclear charge [13]. Coherence plays a most important role in neutrino dynamics within supernovae and neutron stars [1], adding to the attraction of a laboratory measurement. In particular, a measurement of the total (flavor-independent) neutrino flux from a nearby supernova using a massive enough coherent detector would be of capital importance to help clarify the exact oscillation pattern followed by the neutrinos in their way to the Earth [14].

2. A first coherent neutrino detector

The low background detector development group at the Enrico Fermi Institute has investigated several new technologies, each in principle capable of meeting the three goals (energy threshold, background and minimum detector mass) required for a successful measurement of this mode of neutrino interaction in a power reactor. In this paper we concentrate on what is presently considered the most promising path towards this measurement. The prototype described here exhibits an active mass of 475 g, sufficient for a measurement of the cross-section. The technology is however readily scalable to a mass $O(10)$ kg, necessary for most of the applications mentioned above, in the form of a small array of detectors.

While an average of 20–100 eV in deposited ionization energy is required to generate a signal carrier (electron, photon) in proportional chambers or scintillating particle detectors, semiconductors offer the same for a ~ 3 eV modicum. It would then make sense to examine the possibility of using large intrinsic germanium detectors for this application. Unfortunately, the large capacitance of a germanium diode of this mass (~ 1 kg) results in prohibitive electronic noise levels, i.e., ionization energy thresholds of a few kiloelectronvolt. When a low energy quenching factor for Ge recoils of $O(20)\%$ [15] is taken into consideration, the situation is seen to be hopeless for any artificial low energy neutrino source. The TEXONO collaboration has recently proposed [16] to bypass this impediment by using arrays of commercially available smaller n-type germanium diodes (5 g) where the low capacitance (~ 1 pF) results in ~ 300 eV hardware ionization thresholds. In those conditions, as discussed below, coherent signal rates of $O(10)$ detectable recoils $\text{kg}^{-1} \text{day}^{-1}$ are possible from power reactors. The drawbacks of that approach are evident: a single kilogram of target mass requires a multitude of amplification channels and a large monetary investment. Near threshold, a much higher rate of unrejectable electronic noise-induced events per unit mass would be sustained than in a single-channel 1 kg crystal of comparable threshold, if such a thing could be built. Finally, the unfavorable peak-to-Compton ratio for detectors this small results in partial energy depositions from environmental radioactive backgrounds being strongly favored, swamping the signal region [16].

Large germanium detectors with < 1 pF capacitance and ~ 1 kg of mass can be built, and this is the approach taken here. Modifications of the usual electrode structure in a variety of detector geometries [17]–[19] can lead to these uncommonly low values of the capacitance, in some cases at the expense of degraded energy resolutions, which are evidently not the biggest issue in the present application (the intrinsically low resolution

for small energy depositions being more important). An 800 g modified coaxial detector with a n^+ central electrode (n-type) just 1 mm in radius and 0.5 mm deep achieved a 270 eV FWHM noise level [19], a sizable improvement over a standard coaxial detector of the same mass. The measured capacitance (1 pF) was in excellent agreement with expectations based on the chosen electrode geometry [19]. In order for the carriers to be efficiently collected along the axis of such a detector a gradient of impurities in the crystal must be present for space-charge effects to establish an effective electric field in this direction. Material with these characteristics is actually commonly present in germanium ingots as a result of segregation processes during crystal growth [20]. The detector in [19] was inspired by searches for the ‘cosmion’ [21], a low mass particle dark matter candidate thought at the time to be able to explain the now defunct ‘solar neutrino problem’. Due to their light mass (~ 1 GeV) these particles were expected to produce relatively soft recoils. Cosmions were experimentally ruled out soon after and no further progress nor interest in these detectors appears in the literature.

A noise level of 270 eV (resulting in a threshold two to three times higher) would still be insufficient for a reactor experiment looking for coherent neutrino scattering. However, a number of improvements could in principle reduce this to a threshold ~ 100 eV or even lower in such a large detector, which would yield a comfortable signal rate for present purposes. Since a large fraction of the noise figure in [19] was due to the electronic characteristics of the field effect transistors (JFETs) available 20 years ago, it seemed timely to reconsider this approach in the light of the most recent technology. A number of possible improvements were envisioned:

- Replacing the resistor-feedback preamplifier used in [19] by a lower noise optical- or transistor-reset type is observed to reduce on its own the electronic noise level by a factor ~ 2 [22] in detectors with a capacitance $C_D \sim 1$ pF using the same JFET as in [19] (Texas Instruments 2N4416). This is at the expense of a reduced energy throughput [22], which is however not a concern in low counting rate experiments.
- Great progress in reducing JFET capacitance (C_F) and noise voltage (V_n) has taken place since [19]. The 2N4416 JFET is now fully outdated [23] ($C_F = 4.2$ pF, $V_n = 2$ nV Hz $^{-1/2}$ at 295 K and 10 kHz). A state-of-the-art EurifET ER105 ($C_F = 0.9$ pF, $V_n = 1.6$ nV/ $\sqrt{\text{Hz}}$ at 295 K and 10 kHz), proprietary to CANBERRA Industries, provides a perfect capacitance match to a $C_D \sim 1$ pF and in the process the theoretically best possible signal-to-noise ratio [24, 25]. The electronic noise level (as described by the energy resolution using a pulser) that can be expected from these technological improvements is described for germanium by the expression [25, 26]:

$$\text{FWHM} = (41 \text{ eV})V_n(C_F + C_D)/\sqrt{\Delta t}, \quad (1)$$

with all units as above and Δt (μs) being the shaping (integration) time of the (second stage) spectroscopy amplifier. For $\Delta t = 8 \mu\text{s}$ as in [19], an optimal ~ 45 eV FWHM is to be expected, in contrast to ~ 130 eV for the 2N4416 (this last figure in fair agreement with the observations in [19] after introducing the factor ~ 2 noise increase from the resistor-feedback preamplifier). This noise figure is precisely at the level of the very best performance presently achievable with small $C_D = 1$ pF, low C_F , low V_n silicon x-ray detectors [23, 26]: the conclusion is that, in principle, it could also be achieved with a modified electrode large-mass HPGe detector. These

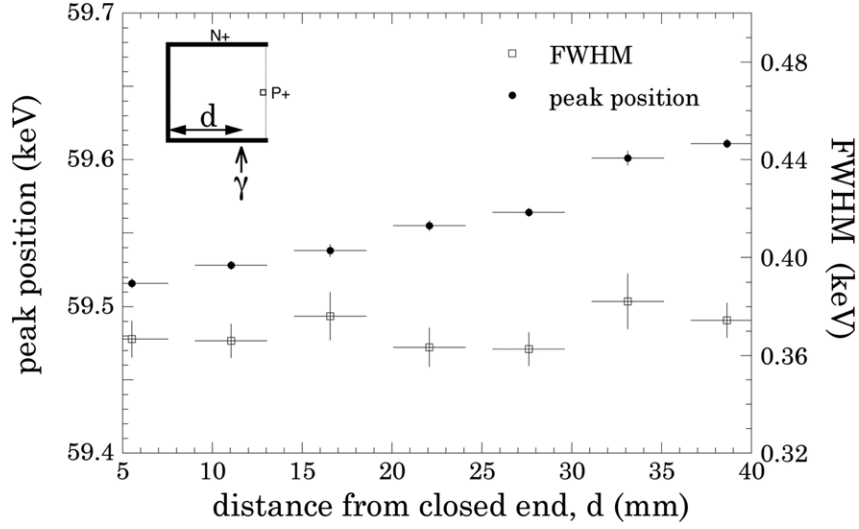


Figure 1. Energy resolution (FWHM) and effective gain shift observed using low energy gamma emissions from a collimated ^{241}Am source at different positions along the longitudinal HPGe crystal axis. The tiny axial dependence of the second (0.15% maximum variation) demonstrates an optimal charge collection even in the presence of a modified electrode configuration.

promising expectations may nevertheless be somewhat limited by the effect of lossy dielectrics [27] and leakage currents [28], which are seen to start to dominate noise contributions precisely at the scale of 50 eV FWHM (see discussion below). It is nevertheless worth mentioning that JFET technology continues to improve, and that experimental $C_F = 0.4$ pF proprietary JFETs are available to CANBERRA Industries. This represents a full order of magnitude improvement since [19].

Motivated by this potential for progress and aiming at obtaining detector specifications sufficient for a demonstration measurement of the coherent neutrino–nucleus scattering cross-section, a modified electrode HPGe detector was built by CANBERRA Industries during 2005. Besides the mentioned improvements to the electronics, another critical departure from the approach described in [19] was the choice of p-type rather than n-type electrode configuration. A first evident reason for this was to enjoy a diminished sensitivity to very low energy minimum ionizing backgrounds (surface betas, x-rays, etc), profiting from the ~ 0.5 mm deep dead layer imposed by the n+ lithium-drifted contact that spans most of the surface of a p-type HPGe. The second was to avoid the crippling degradation in the energy resolution of the detector in [19], which can be ascribed to electron trapping in dislocations as they travel relatively long distances through the crystal to the n+ central electrode in that geometry. It is for this reason that p-type detectors generally exhibit better charge collection than n-type, and this was deemed especially important given the poor drift fields encountered with a modified electrode geometry. As discussed below, obtaining an optimal energy resolution is of crucial importance for some of the detector applications envisioned.

The prototype displays an energy resolution (measured with a pulser) of 140 eV FWHM and a charge collection (figure 1) comparable to that from a conventional coaxial

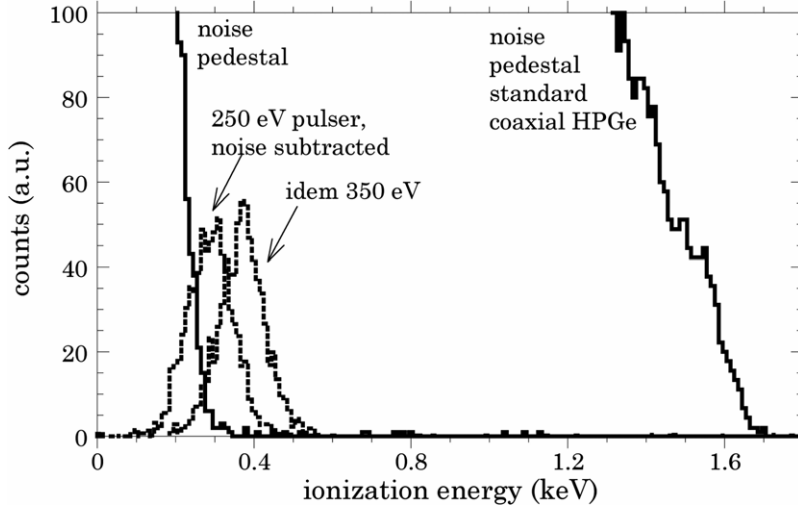


Figure 2. A comparison of the energy threshold (~ 330 eV, five sigma from noise centroid) in the modified electrode HPGe with that of a conventional coaxial detector of the same mass (~ 475 g), typically in the few kiloelectronvolt region (the particular one used for the figure being relatively low in noise). No instabilities in the threshold have been observed in five months of continuous detector operation. Energies are electron equivalent, i.e., ionization.

electrode HPGe. To put its performance in perspective, besides a much reduced noise level and threshold, it shows an enhancement in energy resolution from a much degraded value of ~ 15 FWHM (^{60}Co , 1.33 MeV) measured in [19] to a 1.82 keV FWHM, typical of a modern large coaxial HPGe. Charge collection uniformity along the axis varies by less than 0.15% (figure 1), compared to 3% in [19]. In other words, the device has the mass (475 g) and energy resolution typical of a large HPGe gamma spectrometer while simultaneously displaying the low noise and low energy threshold (figure 2) of an x-ray detector a hundred times lighter. This unique combination makes the device a first of a kind, opening up a number of other interesting applications discussed in section 3. It is the first time that such a combination of mass, energy threshold and resolution has been produced in a detector of any kind.

From the point of view of target mass and sensitivity to very small energy depositions the device is ready for a measurement of coherent neutrino scattering in a reactor experiment: the inset in figure 3 displays the fraction of recoils above a choice of three different ionization energy thresholds E_{thr} (i.e., the fraction of detectable events) as a function of their deposited (ionization) energy. The dotted line corresponds to pulser measurements (black dots) using this prototype ($E_{\text{thr}} = 330$ eV). To make these measurements possible, a careful energy calibration of the pulser was performed with the help of five gamma and x-ray lines identifiable in shielded conditions over the range 10–100 keV. The dashed line corresponds to envisioned minimal upgrades to the JFET (see below), resulting in $E_{\text{thr}} = 200$ eV. The dash-dotted line illustrates the ultimate performance ($E_{\text{thr}} \sim 100$ eV) that can be expected with present-day JFET technology, matching the state-of-the-art in low noise x-ray detectors [23, 26]. The combined effect of threshold and energy resolution can then be folded into the expected differential recoil rate

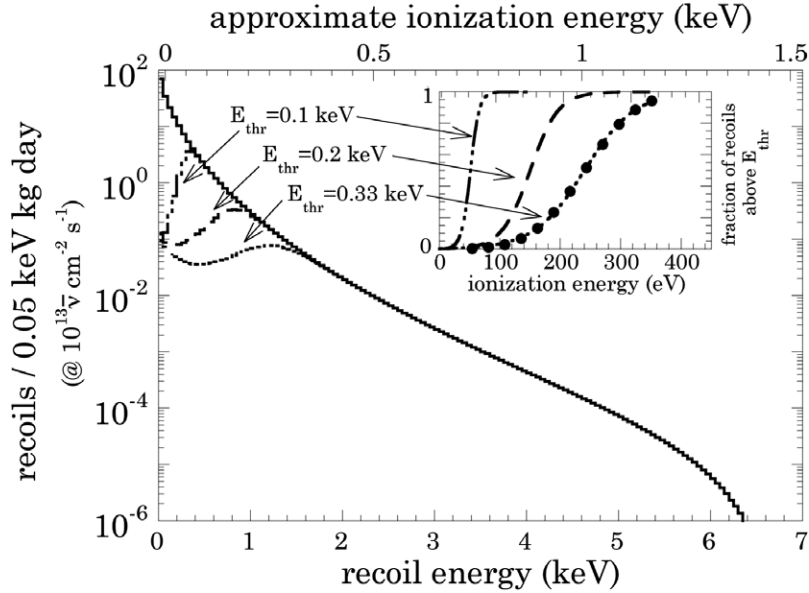


Figure 3. Effect of detector threshold and energy resolution in the differential rate of recoils expected from reactor antineutrinos (see text).

in a reactor experiment (main plot, figure 3), leading to integrated detectable coherent scattering rates of ~ 2.5 , ~ 6 and ~ 28 events $\text{kg}^{-1} \text{day}^{-1}$, respectively.

The quenching factor used for these calculations is the standard Lindhard theory prediction for Ge ($k = 0.2$ in the notation of [15]). Measurements of this quenching factor in the interval of recoil energies 0.3–1.4 keV have been recently performed at the dedicated neutron beam described in a companion paper [6], using the existing prototype. While the many details of the analysis must be necessarily reserved for another publication [31], figure 4 illustrates the main results from this essential calibration, showing an excellent agreement with Lindhard-based expectations. It must be emphasized that the same range of recoil energies relevant to the upcoming reactor experiment (figure 5) has been explored in this calibration (figure 4), a crucial requirement before embarking in such a delicate measurement. To our knowledge, it is the first time that recoils this low in energy are directly and individually recorded (the measurements in [15] are indirect, i.e., based on the sum of recoil energy and a 69 keV nuclear de-excitation gamma).

Statistical evidence for coherent scattering can be gathered with the present prototype within just a few months of data acquisition near a power reactor, once the background goal depicted in figure 5 is reached. The disappearance of the neutrino signal during the refueling of the reactor (spanning 1–3 months every 12–18 months) would confirm the measurement. Shielded runs at a depth of 6 mwe and extensive MCNP4b simulations [32] of U, Th, and ^{40}K gamma and beta emissions in preamplifier parts, crystal holder and endcap indicate that the projected level of background is reachable with adequate active and passive gamma and neutron shielding in combination with a NaI(Tl) anti-Compton shield (figure 6). At least two precedents exist [33] for achieving $\text{O}(1)$ count $\text{keV}^{-1} \text{kg}^{-1} \text{day}^{-1}$ in the few kiloelectronvolt region while benefiting from just a shallow (few mwe) overburden, what is expected at best in a reactor site (e.g., in

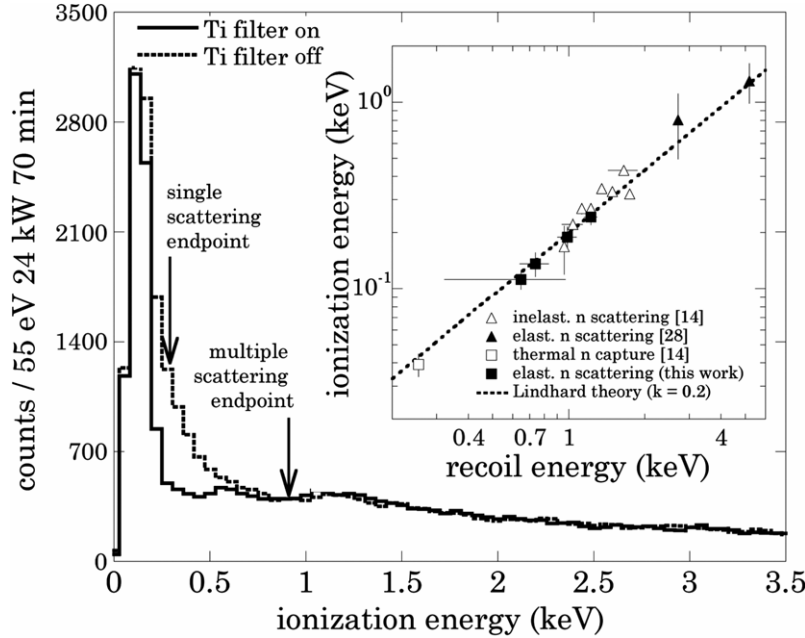


Figure 4. Exposure of the prototype to a monochromatic 24 keV reactor neutron beam custom-built to mimic reactor antineutrino recoils [6]. A titanium postfilter allows to switch off the dominant 24 keV beam component and with it the neutrino-like recoils, leaving the scarce backgrounds intact [6]. To illustrate its effect, the vertical arrows mark the energy at which the endpoint of these soft recoils is predicted, based on a full MCNP-Polimi simulation [29] of the experiment and the expected 20% quenching factor. Inset: signals time-coincident with the thermal peak of a large $^6\text{LiI}[\text{Eu}]$ scintillator mounted on a goniometric table allow to select discrete Ge recoil energies, for which quenching factors can then be obtained [6]. An excellent agreement with Lindhard theory expectations has been observed over the range of recoil energies relevant to the upcoming reactor neutrino experiment (see text).

a ‘tendon’ gallery ~ 20 m from the core [34]). An important source of non-radioactive background in the low energy region is microphonic noise: pulse shape discrimination (PSD) techniques (analog [35] and digital [36]) can be applied against it. With the single precautions of vibration-absorbing pads under the Dewar and attention to mechanically decoupling the cryostat from shielding materials, the prototype is observed to be rather insensitive to these (figure 7). This is possibly a result of the very small capacitances involved [37].

It is worth emphasizing that contrary to what is implied in [16], PSD techniques alone cannot be used to reduce an energy threshold imposed by electronic noise, unless an inadmissible penalty in signal acceptance is paid. In other words, any PSD cuts must be justified on grounds of clear physical differences between signal and noise pulses, as in [35]. Figure 7 illustrates the indistinguishability of most true signals and noise below threshold. Concentration should be in reducing electronic noise at the hardware level. Towards this end, the noise components in this prototype have been characterized. As evidenced in the discussion of figure 3 the technique has not yet met the limitations imposed by present-day

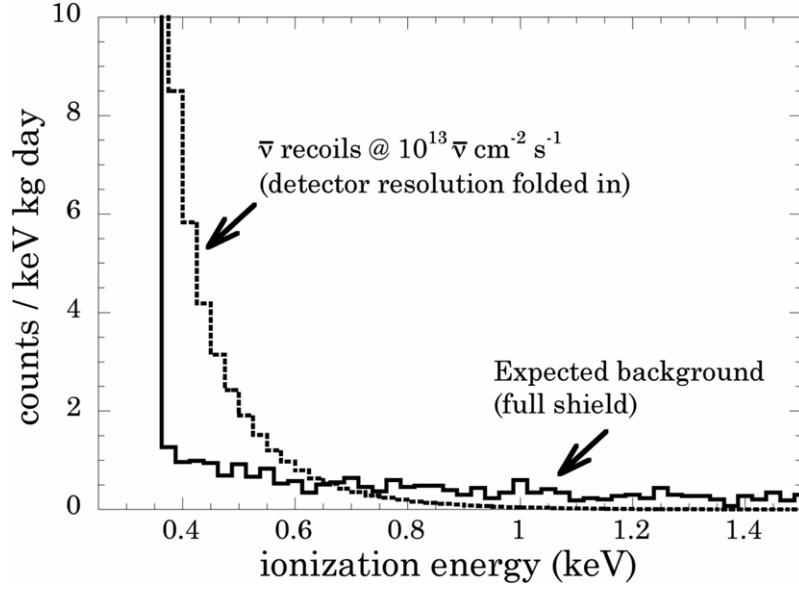


Figure 5. Expected antineutrino signal in the planned demonstration reactor experiment, clearly visible above the background goal. The relevant region of interest in recoil energy has been explored during dedicated neutron calibrations (figure 4). The background is scaled down from data acquired with a partial shielding in place, i.e., the spectral shape depicted is representative of actual observations.

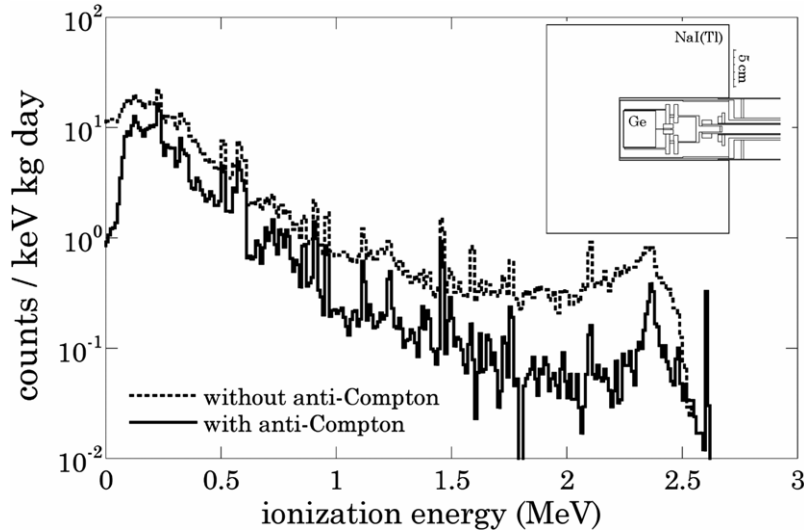


Figure 6. Simulated effect of the anti-Compton veto in reducing the dominant contribution from radiocontamination in the preamplifier components (~ 4 Bq ^{238}U , ~ 6.5 Bq ^{232}Th , ~ 0.2 Bq ^{40}K).

JFET technology: a threshold lower by a factor of ~ 3 should be presently feasible with further effort, leading to a >10 enhancement in the signal rate per kilogram of detector mass for this neutrino process. An analysis of the electronic noise components in the existing prototype (figure 8) indicates that while the expectations described above for the series component have been met (i.e., noise determined by the JFET and detector

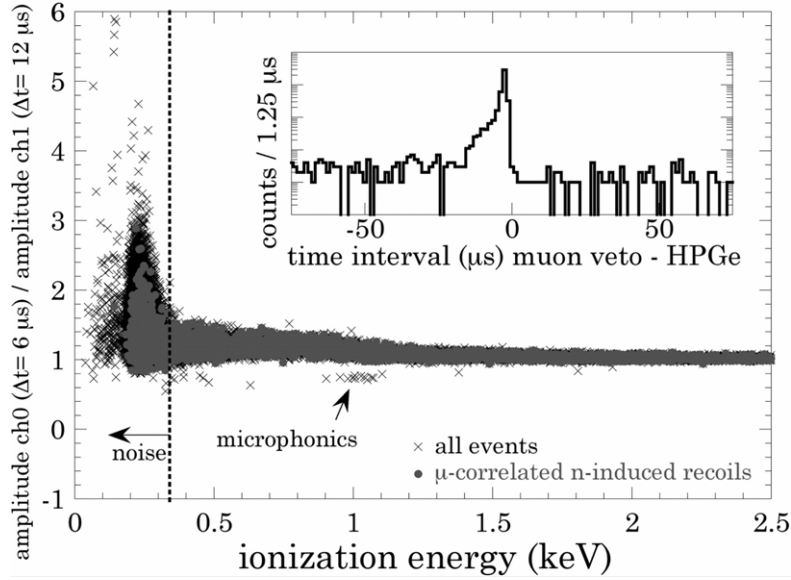


Figure 7. Application of an analog method to reject anomalous pulses such as microphonics [35] in the energy region near the detector threshold. Low energy nuclear recoils produced by veto-tagged muon-induced neutrons (inset), characteristically delayed by the few microsecond of neutron straggling, are used to generate a template of ‘good’ low energy events (solid dots). Only a scarce number of microphonic events and a small fraction of electronic noise below threshold are observed to clearly deviate from it.

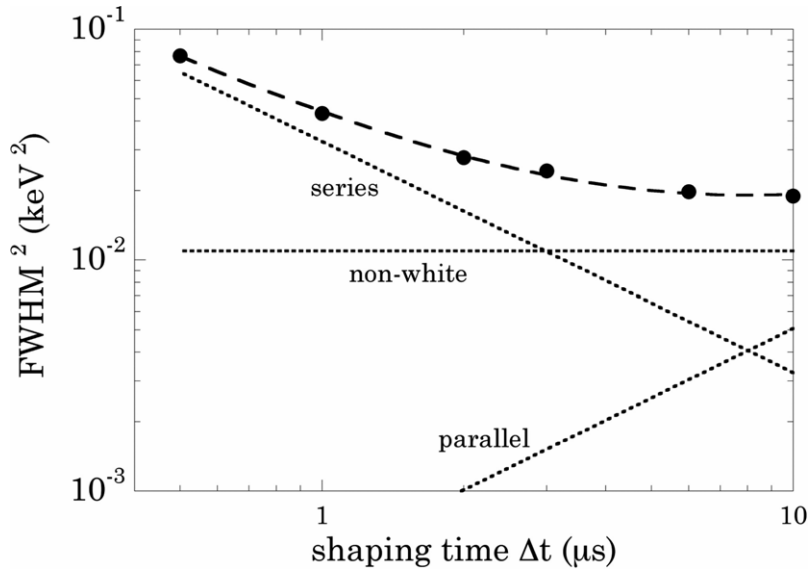


Figure 8. Measured electronic noise components in the prototype (see text).

capacitances, equation (1), a non-white component presently dominates. The origin of this is generally traceable to lossy dielectrics. Rearrangement and selection of the JFET package components should be able to lower this component to more manageable levels [38] and to generate an electronic noise behavior truly comparable to that of the best ~ 1 pF

x-ray detectors presently available. A small decrease in leakage current would also benefit the parallel noise component, leading to the (presently) ultimate performance, i.e., few tens of detectable recoils per kilogram of Ge per day in the vicinity (~ 20 m) of a high power reactor. We note that up to an additional order of magnitude in signal rate could be obtained from a dedicated effort to reduce noise levels beyond the present state-of-the-art.

While the detection of this intriguing mode of neutrino interaction seems finally within reach, many applications, either technological or in the study of fundamental neutrino properties would need to involve small arrays (~ 10 elements) of these detectors: such HPGe clusters are common nowadays [39]. Recent advances in HPGe detector encapsulation [40] (leading to simplified handling and enhanced stability of array elements) and microphonic-free cryocooling of HPGe arrays [41] can be applied to the construction of truly *compact* coherent neutrino detectors comprised of a modest number of modified electrode crystals. In the specific realm of reactor monitoring applications, their sensitivity (hundreds of events per day) would then rival more cumbersome approaches based on underground ton-sized scintillator tanks [8, 34].

3. Applications beyond coherent neutrino scattering

The interest of a large-mass, ultralow threshold semiconductor detector is not limited to coherent neutrino detection. Experimental searches for weakly interacting massive particles (WIMPs) [42], prime dark matter particle candidates, typically assume that these particles are gravitationally bound to our galaxy, resulting in expected speeds relative to Earth of $O(300)$ km s $^{-1}$. This in turn determines the recoil energies they are to deposit in dedicated detectors (few kiloelectronvolt to tens of kiloelectronvolt, depending on their mass). An alternative WIMP population consists of those that fell into stable closed solar orbits during the formation of the protosolar nebula, following collisionless mechanisms [43]. In that case their maximum speed is limited by the escape velocity from the sun at Earth (42 km s $^{-1}$), leading to a large concentration of the recoil signal below the threshold of present-day WIMP detectors [44] but now within reach of this new device. A second assumption driving most WIMP searches is the false tenet that the only supersymmetric WIMP candidate is the so-called neutralino [42]: as has been recently emphasized [45], a parallel phenomenology exists for other non-pointlike supersymmetric dark matter candidates (e.g., Q -balls), one that involves very soft recoils, again generally below threshold and hence beyond detection for more conventional detector designs. A third application in this field of dark matter detection is the exploration of the possibility that a light (5–12 GeV c $^{-2}$) particle might be responsible for the controversial WIMP DAMA signal [46], a hypothesis not contradicted yet by any other experiments [47]–[49] (figure 9). While light neutralinos with masses below ~ 20 GeV c $^{-2}$ are strongly favored by the next-to-minimal supersymmetric standard model (NMSSM) [50, 51], they remain beyond the reach of conventional WIMP detectors. The first experimental limits on these interesting possibilities can be extracted from background characterization runs for the existing prototype [31], with a sensitivity that should increase as the technique is further developed (figure 10). Ironically, WIMP interaction rates like those in figure 9 would complicate or even frustrate any attempt to detect reactor neutrinos coherently. Separately from the subject of dark matter searches, it is also worth remembering that the present sensitivity to a finite neutrino magnetic moment should be increased by

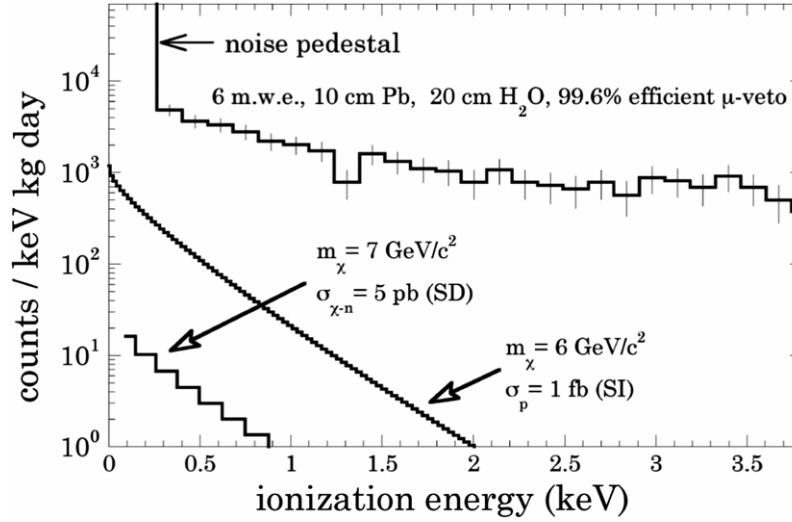


Figure 9. Signals expected from typical WIMP candidates able to explain the DAMA annual modulation [46] while satisfying the limits imposed by all other experiments [47, 48]. The differential spectra are labelled by WIMP mass and proton cross-section (SI = spin-independent coupling, SD = spin-dependent type). The prototype data were acquired with a partial shield. The addition of a NaI anti-Compton veto (expected $\times 10$ reduction in background), replacement of cryostat endcap and crystal holder with low activity Al ($\times 50$ reduction) and additional Pb and overburden should allow to confirm or rule out these light dark matter candidates.

about an order of magnitude, down to $\mu_\nu(\bar{\nu}_e) \rightarrow \sim 2 \times 10^{-11} \mu_B$ in a detector with these characteristics [57].

Another important application of a modified electrode HPGe arises from exploiting the characteristic temporal features of the preamplifier traces in this electrode configuration, features already noted in [19]: figure 11 displays two sets of traces, the top panel for a conventional coaxial electrode detector, the bottom panel for the prototype under discussion, both crystals roughly the same mass and dimensions. The top trace in each panel corresponds to the preamplifier output, the bottom one is this same passed through a timing filter amplifier (TFA) set at 10 ns differentiation and 10 ns integration time. Such a TFA trace is a good representation of the time structure of the arrival of charge to the collecting electrodes [36] (the same signal processing can be achieved on software using digitized preamplifier traces). For both detectors the event that originated the pulses was a multiple-site gamma interaction. In the coaxial TFA trace this is barely evident, a double ‘hump’ or somewhat broadened trace being the only signature, resulting in a limited ability to differentiate multiple-site from single-site interactions [36]. In the present prototype however, the longer distances that charge (holes in this case) must travel to the small p+ electrode result in traces generally stretched by a factor ~ 5 in time, yielding a clear separation of individual site contributions to the overall pulse (a three, possibly four-site interaction in the figure). It is worth noting that the reduced electronic noise is in itself an advantage in this type of pulse shape analysis [24]. The insets in figure 11 graphically illustrate how the radial degeneracy imposed by the coaxial

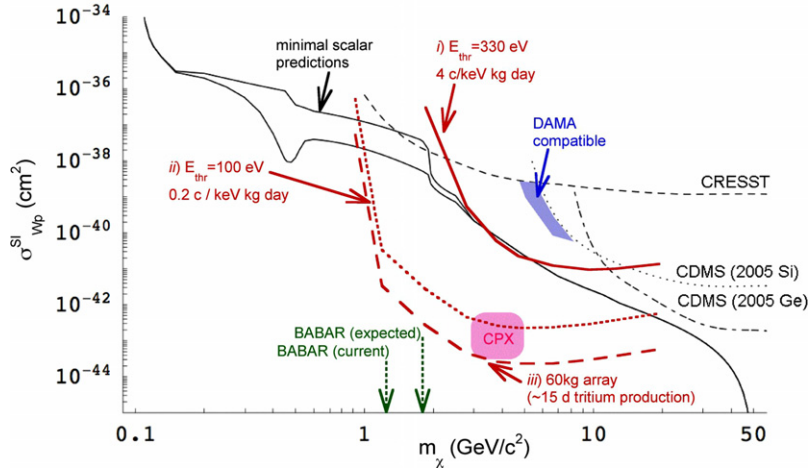


Figure 10. Minimal scalar model predictions for spin-independent WIMP couplings (dark solid lines), displayed together with the threshold-limited sensitivity of present detector technologies (dashed dark lines) [51]. Vertical arrows indicate accelerator lower bounds on the mass of a light neutralino generated by such models [51]. The approximate region of parameter space able to explain the DAMA modulation and not yet excluded by other experiments is also shown (blue patch) [48]. The expected sensitivity of a p-type modified electrode HPGGe detector is indicated by red lines, for different scenarios: (i) present energy threshold and installation in a shallow underground site (300 mwe) after replacement of aluminum cryostat and addition of anti-Compton shield [31], (ii) improved energy threshold closer to the state-of-the-art in low noise FET electronics and a low energy background matching the best achieved with conventional HPGGe detectors in deep underground sites [52], (iii) a MAJORANA-like array limited by the low energy background from cosmogenic tritium production [53]. The region labelled ‘CPX’ corresponds to candidates predicted in [54]. Light candidates like those described in [55] should have couplings in the range between 10^{-41} and 10^{-46} cm^2 [56]. An exhaustive exploration of the WIMP mass region 1–10 $\text{GeV } c^{-2}$, complementary to accelerator and conventional WIMP searches is within reach.

electrode dissolves for the modified electrode: in the first case, the trajectories along the dashed field lines followed by electrons and holes generated at similar radial distances in the crystal are comparable, leading to a trace that would most probably be misidentified as corresponding to a single-site interaction. In the second, for the same initial distribution of charge, the hole trajectories are considerably different, leading to positive identification of the event as a multi-site interaction. In figure 12 this effect is illustrated with the help of a 59.5 keV ^{241}Am collimated gamma source impinging on the crystal perpendicularly to its axis and, given the low gamma energy, interacting via single-site photoelectric effect very close to the surface. Little difference is observed as a function of axial source position in coaxial traces (top), whereas the prototype traces (bottom) are clearly rich in position information. In this respect and as a simple curiosity, keeping in mind that the charge drift speed in depleted Ge is ~ 10 $\text{ns } \text{mm}^{-1}$, it is possible to extract the rough crystal radius (2.5 cm in actuality) from the rise time of the $d = 43$ mm trace (the closest gamma

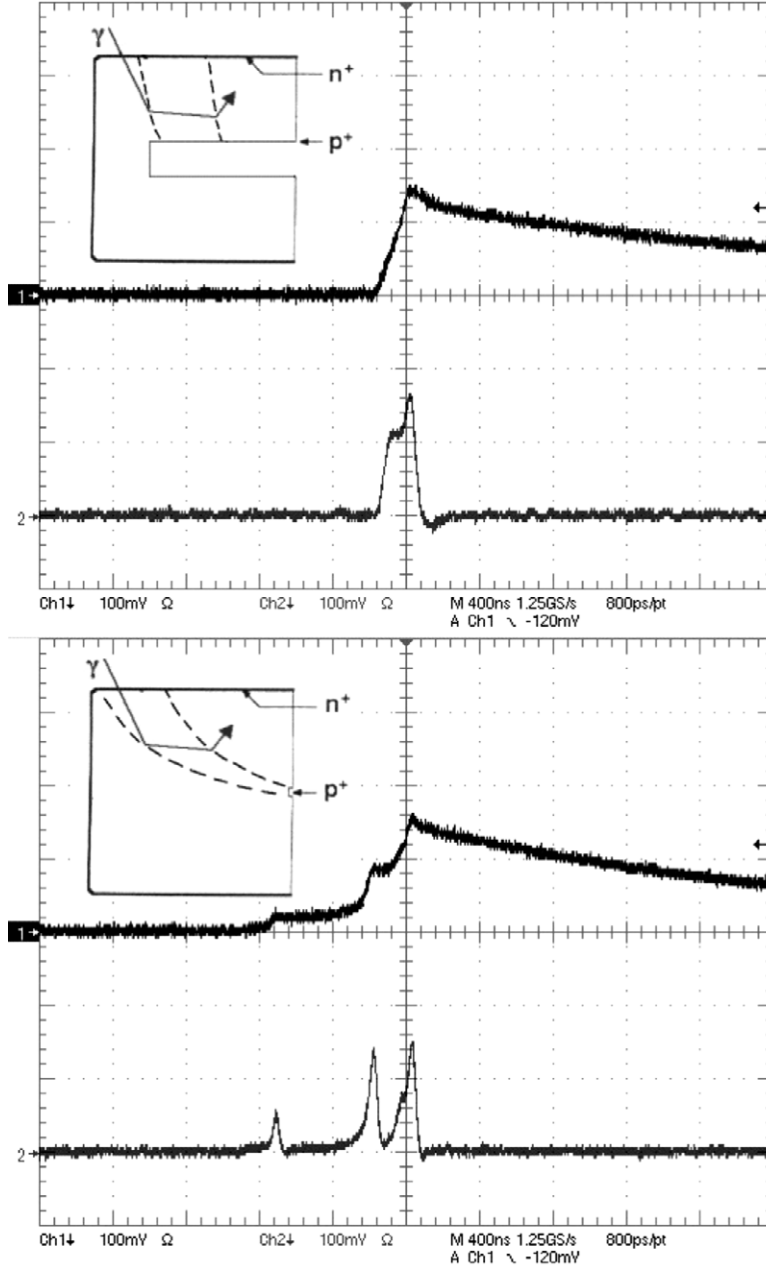


Figure 11. Effect of electrode geometry on pulse formation for a multiple-site gamma interaction (see text).

injection point to the p+ electrode, at the base of the crystal), as well as the approximate crystal length (4.4 cm) from the time dispersion in the onset of the traces.

Besides the evident commercial applications that distinguishing single-site from multiple-site interactions might have (e.g., an effective higher peak-to-Compton ratio for smallish crystals), next-generation neutrinoless double-beta decay searches using germanium crystals as source and target (MAJORANA [58], GERDA [59]) rely heavily on this distinction: the process of interest, the local emission of two short-ranged ~ 1 MeV

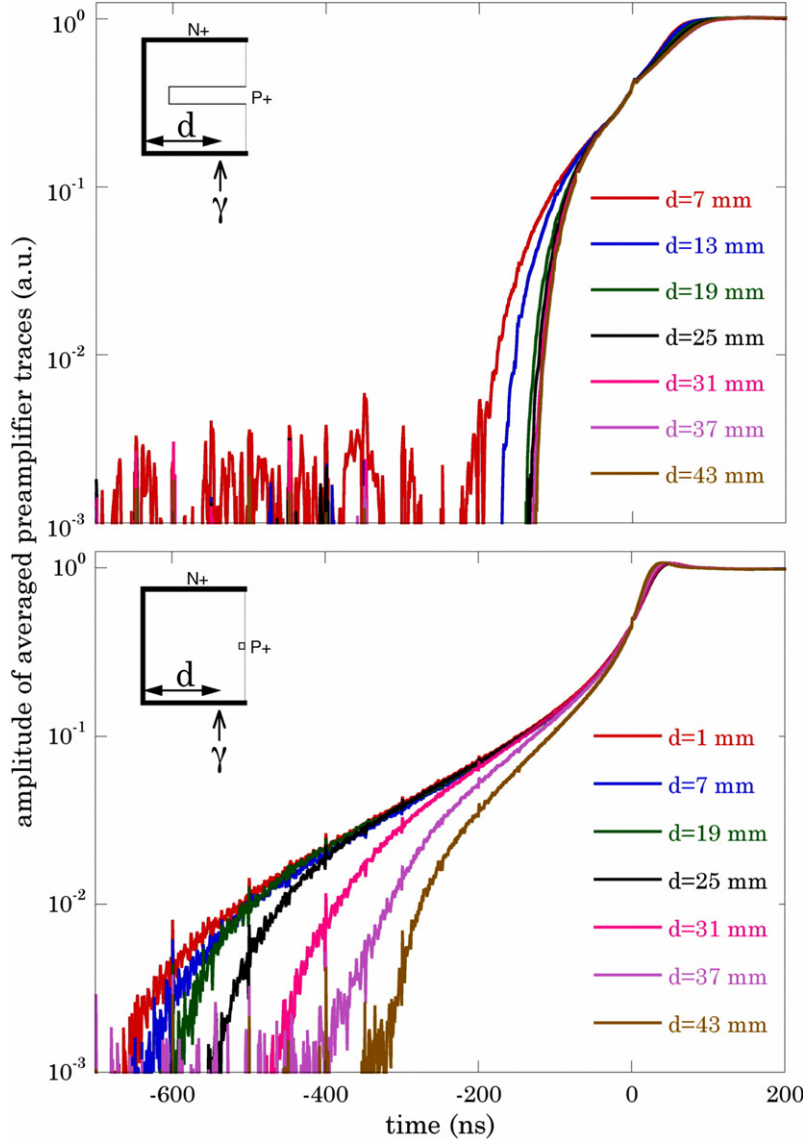


Figure 12. Normalized preamplifier rising edges for a coaxial (top) and modified electrode (bottom) HPGe (see text).

electrons indicating a neutrinoless decay, is eminently single-site type, while a large fraction of backgrounds is not. The mentioned limited performance in this respect from conventional coaxial crystals has led these experimental efforts to consider complex multi-electrode segmented germanium detectors, where the additional spatial granularity helps improve the background rejection ability. Evidently, the prohibitive energy resolution degradation observed in n-type modified electrode schemes [19] would never allow one to consider a neutrinoless double-beta decay application, where the signature sought is a very precisely defined energy deposition corresponding to the Q -value of the nuclear transition (2039 keV for ^{76}Ge). The optimal charge collection observed in a p-type design leads on the other hand to excellent prospects. Figure 13 shows the results of a prototype irradiation with a natural Th source. Following [60], the ^{228}Ac gamma ray at 1588 keV

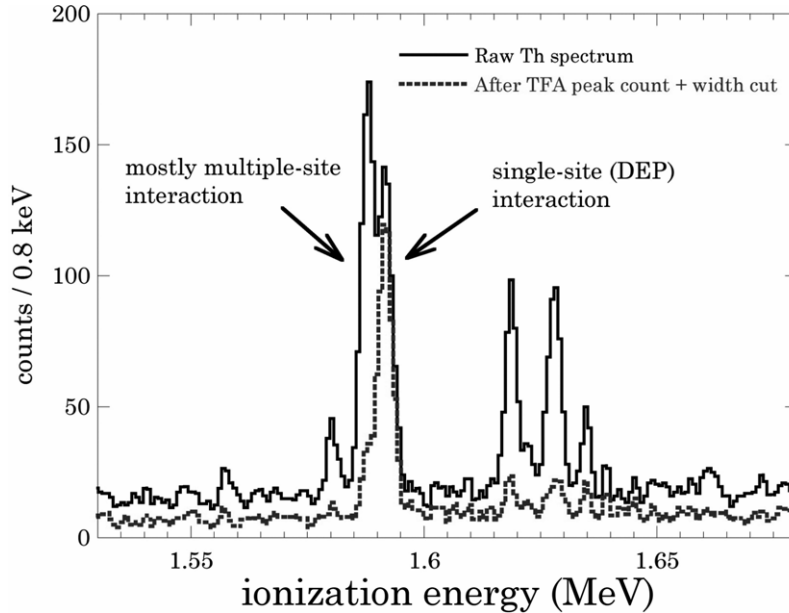


Figure 13. Natural thorium irradiation of the modified electrode p-type detector and effect of PSD cuts on rejection of multiple-site events (see text). The energy resolution appears slightly degraded due to the limited resolution of the digitizer employed (8 bit).

typically interacts three times to deposit its full energy, whereas the line at 1592 keV arises from a double escape (i.e., a single interaction) from a 2614 keV emission in ^{208}Tl . Their neighboring energies provide a convenient benchmark to assess the ability of a detector to distinguish single-site from multiple-site interactions [60]. A simple, energy-independent set of cuts based on peak counting of digitized TFA traces such as those in figure 11 leads to a background (multiple-site) rejection (BR) of 88% for a signal acceptance (SA) of 93% (figure 13). This compares very favorably, even prior to the beneficial effect of close-packing crystals, to an eight-channel segmented four-crystal ‘clover’ HPGe detector (93% BR for 73% SA) and a single n-type 18-segment detector (65% BR for 92% SA) [61]. In the case of the modified electrode prototype, application of the same cuts to the neutrinoless double-beta decay region of interest (2.04 MeV) leads to a reduction in background by $\sim 50\%$, in close agreement with the expectations from a simulation of this particular Th irradiation. In other words, the bulk of multiple-site backgrounds is successfully rejected.

Besides the obvious advantages that use of a single-channel device can bring to next-generation germanium double-beta decay searches (increased speed of deployment, reduction in costs, simplified construction and analysis) there are other more subtle ones that can be listed: first, the largest fraction of the backgrounds is expected to arise from front-end electronics and their cabling, evidently much more numerous in a segmented detector approach. Second, the thermal load imposed by the excess cabling involved in segmented schemes is much reduced. Third, long-term instabilities and channel cross-talk are known undesirable features in some segmented configurations. Fourth, segmentation schemes involve use of n-type crystals: leaving aside the slightly lesser energy resolution these usually display (however crucial in the double-beta case), p-type crystals are more

rugged, which is advantageous when arraying. They should also profit from the thick lithium-drifted dead layer to exhibit a much lower sensitivity to surface contaminations, implanted and absorbed alpha-emitting Rn daughters being a major concern in double-beta decay experiments.

4. Conclusions

A novel type of radiation detector, a large-mass p-type modified electrode HPGe diode, has been presented. It features an unprecedented combination of sensitivity to small energy depositions, excellent energy resolution, large mass and built-in information about site multiplicity of the interactions: as is often the case, a promising new addition to the existing arsenal of radiation detection technologies can generate a number of exciting applications. In this case, the device can be considered a first viable coherent neutrino detector, allowing us to realistically consider the possible technological applications that smallish neutrino detectors may one day find. In addition to this, a strong role in double-beta decay, neutrino magnetic moment and novel dark matter searches can be foreseen.

Acknowledgments

This work was supported by NSF CAREER award PHY-0239812, DOE/NNSA grant DE-FG52-0-5NA25686, and in part by the Kavli Institute for Cosmological Physics through grant NSF PHY-0114422 and a Research Innovation Award No. RI0917 (Research Corporation). We are indebted to J Lenhart and T Wilson at NNSA/NA-22 for their constant support of this project and to L Darken and D Gutknecht for their contributions to the crystal growing and detector fabrication. Similarly, to C Aalseth, F T Avignone, J Beacom, R L Brodzinski, G Gelmini, P Gondolo, A Kusenko, P Luke, H S Miley, B Odom, D Radford, J Wilkerson and the MAJORANA collaboration for many useful exchanges. This work is dedicated to the memory of R L Brodzinski.

References

- [1] Freedman D Z *et al*, 1977 *Ann. Rev. Nucl. Part. Sci.* **27** 167 [SPIRES]
- [2] Drukier A and Stodolsky L, 1984 *Phys. Rev. D* **30** 2295 [SPIRES]
- [3] Angloher G *et al*, 2002 *Astropart. Phys.* **18** 43 [SPIRES]
- [4] Barbeau P S *et al*, 2003 *IEEE Trans. Nucl. Sci.* **50** 1285
- [5] Cabrera B *et al*, 1985 *Phys. Rev. Lett.* **55** 25 [SPIRES]
- Starostin A S and Beda A G, 2000 *Phys. Atom. Nucl.* **63** 1297 [SPIRES]
- Wong H T, 2005 *Nucl. Phys. B (Proc. Suppl.)* **138** 333
- Beda A G, 2004 *Nucl. Instrum. Meth. A* **531** 161 [SPIRES]
- Hagmann C and Bernstein A, 2004 *IEEE Trans. Nucl. Sci.* **51** 2151
- Giomataris I *et al*, 2005 Preprint [hep-ex/0502033](http://arxiv.org/abs/hep-ex/0502033)
- S A Golubkov *et al*, 2004 *Instr. Exp. Tech.* **47** 799
- Scholberg K, 2006 *Phys. Rev. D* **73** 033005 [SPIRES]
- Braggio C *et al*, 2006 *Nucl. Instrum. Meth. A* **568** 412 [SPIRES]
- Bueno A *et al*, 2006 *Phys. Rev. D* **74** 033010 [SPIRES]
- Bondar A *et al*, 2006 Preprint [physics/0611068](http://arxiv.org/abs/physics/0611068)
- [6] Barbeau P S *et al*, *Design and characterization of a neutron calibration facility for the study of sub-keV nuclear recoils*, 2007 *Nucl. Instrum. Meth. A* **574** 385 [SPIRES] [[nucl-ex/0701011](http://arxiv.org/abs/nucl-ex/0701011)]
- [7] See L Stodolsky's presentation in <http://www.mpa-garching.mpg.de/SFB/ringberg-1997/>
- [8] Bernstein A *et al*, 2001 Preprint [nucl-ex/0108001](http://arxiv.org/abs/nucl-ex/0108001)
- Nieto M M *et al*, 2005 *Nucl. Sci. Eng.* **149** 270

- Nieto M M *et al*, *Procs. of the 2006 Applied Antineutrino Physics Workshop (Livermore, CA, 24–26 Sept. 2006)* available from <http://neutrinos.llnl.gov/workshop/aap2006.html>
- [9] Sehgal L M, 1985 *Phys. Lett. B* **162** 370 [SPIRES]
- [10] Dodd A C *et al*, 1991 *Phys. Lett. B* **266** 434 [SPIRES]
- [11] Barranco J *et al*, 2005 *J. High Energy Phys.* JHEP12(2005)021 [SPIRES]
- [12] Papavassiliou J *et al*, 2005 Preprint [hep-ph/0512029](http://arxiv.org/abs/hep-ph/0512029)
- [13] Krauss L M, 1991 *Phys. Lett. B* **269** 407 [SPIRES]
- [14] Beacom J F, Farr W M and Vogel P, 2002 *Phys. Rev. D* **66** 033001 [SPIRES]
- [15] Jones K W and Kraner H W, 1975 *Phys. Rev. A* **11** 1347 [SPIRES]
Jones K W and Kraner H W, 1971 *Phys. Rev. C* **4** 125 [SPIRES]
- [16] Wong H T *et al* (TEXONO collaboration), 2005 *Nucl. Phys. B (Proc. Suppl.)* **138** 333
Wong H T *et al* (TEXONO collaboration), 2005 *Nucl. Phys. B (Proc. Suppl.)* **143** 501
- [17] Gatti E and Rehak P, 1984 *Nucl. Instrum. Meth.* **225** 608
Gatti E *et al*, 1984 *Nucl. Instrum. Meth.* **226** 129
Rawlings K J, 1986 *Nucl. Instrum. Meth. A* **253** 85 [SPIRES]
Gatti E *et al*, 1987 *Nucl. Instrum. Meth. A* **253** 511 [SPIRES]
Kemmer J *et al*, 1987 *Nucl. Instrum. Meth. A* **253** 378 [SPIRES]
- [18] Luke P N, Madden N W and Goulding F S, 1985 *IEEE Trans. Nucl. Sci.* **32** 457
Luke P N, 1988 *Nucl. Instrum. Meth. A* **271** 567 [SPIRES]
- [19] Luke P N, Goulding F S, Madden N W and Pehl R H, 1989 *IEEE Trans. Nucl. Sci.* **36** 926
- [20] Haller E E, Hansen W L and Goulding F S, 1981 *Adv. Phys.* **30** 93 [SPIRES]
- [21] Gelmini G B *et al*, 1987 *Nucl. Phys. B* **281** 726 [SPIRES]
- [22] Landis D A, Goulding F S, Pehl R H and Walton J T, 1971 *IEEE Trans. Nucl. Sci.* **18** 115
Landis D A, Goulding F S and Jaklevic J M, 1970 *Nucl. Instrum. Meth.* **87** 211
Goulding F S, Walton J T and Pehl R H, 1970 *IEEE Trans. Nucl. Sci.* **17** 218
- [23] Goulon J *et al*, 2005 *J. Synchrotron Rad.* **12** 57
- [24] Blair J *et al*, 1999 *Nucl. Instrum. Meth. A* **422** 331 [SPIRES]
- [25] Radeka V, 1988 *Ann. Rev. Nucl. Part. Sci.* **38** 217 [SPIRES]
- [26] Nashashibi T and White G, 1990 *IEEE Trans. Nucl. Sci.* **37** 452
Nashashibi T and White G, 1992 *Nucl. Instrum. Meth. A* **322** 551 [SPIRES]
- [27] Radeka V, 1973 *IEEE Trans. Nucl. Sci.* **20** 182
Kern H E, McKenzie J M and McQuaid J H, 1972 *IEEE Trans. Nucl. Sci.* **19** 345
- [28] Hurley J P, Mathiesen J M and Dagragnano V L, 1967 *Nucl. Instrum. Meth.* **57** 109
- [29] Pozzi S A *et al*, 2003 *Nucl. Instrum. Meth. A* **513** 550 [SPIRES]
- [30] Messous Y *et al*, 1995 *Astropart. Phys.* **3** 361 [SPIRES]
- [31] Barbeau P S and Collar J I, 2007 in preparation
- [32] Briesmeister J F (ed), *MCNP, A General Monte Carlo N-Particle Transport Code*, 1993 Los Alamos preprint LA-12625-M
- [33] Li H B *et al*, 2003 *Phys. Rev. Lett.* **90** 131802 [SPIRES]
Beda A G *et al*, 1998 *Phys. Atom. Nucl.* **61** 66 [SPIRES]
- [34] Bernstein A, 2005 *Neutrino Geophysics* University of Hawaii,
<http://www.phys.hawaii.edu/~sdye/hnsc.html> (2006 *Earth, Moon and Planets* **99** (1–4))
- [35] Morales J *et al*, 1992 *Nucl. Instrum. Meth.* **321** 410
- [36] Baudis L *et al*, 1998 *Nucl. Instrum. Meth. A* **418** 348 [SPIRES]
Hellmig J *et al*, 2000 *Nucl. Instrum. Meth.* **455** 638
Petry F *et al*, 1993 *Nucl. Instrum. Meth. A* **332** 107 [SPIRES]
Gonzalez D *et al*, 2003 *Nucl. Instrum. Meth. A* **515** 634 [SPIRES]
- [37] Rashiduzzaman M D *et al*, 1979 *Nucl. Instrum. Meth.* **160** 127
Muggleton A H F, 1972 *Nucl. Instrum. Meth.* **101** 113
- [38] Pullia A *et al*, 1996 *Nucl. Instrum. Meth. A* **380** 1 [SPIRES]
Llacer J and Meier D F, 1977 *IEEE Trans. Nucl. Sci.* **24** 317
- [39] Smith D M, 2002 *Solar Physics* **210** 33
Sangsingkeow P *et al*, 2003 *Nucl. Instrum. Meth. A* **505** 183 [SPIRES]
Mandrou P *et al*, 1997 *Proc. 2nd INTEGRAL Workshop, ESA SP-382* p 591
- [40] Becker J A *et al*, 2003 *Nucl. Instrum. Meth. A* **505** 167 [SPIRES]
Eberth J *et al*, 1996 *Nucl. Instrum. Meth. A* **369** 135 [SPIRES]
- [41] Fritz G, 2006 *Nuclear Spectrometry user's Forum* NPL Teddington, available from
<http://www.npl.co.uk/nsuf/>

- Ross R G *et al*, 2004 *Advances in Cryogenic Engineering: Trans. of the Cryogenic Engineering Conf.* vol 49B, ed J Waynert *et al* pp 1197–203
- Boyle R, 2004 *Cryogenics* **44** 389
- Bathia R S *et al*, 2002 *Cryogenics* **41** 851
- Bathia R S *et al*, 1999 *Cryogenics* **39** 701
- Evans B E *et al*, 1997 *Cryogenics* **37** 695
- [42] Gaitskell R J, 2004 *Ann. Rev. Nucl. Part. Sci.* **54** 315 [SPIRES]
- [43] Steigman G *et al*, 1978 *Astrophys. J.* **83** 1050 [SPIRES]
- [44] Collar J I, 1999 *Phys. Rev. D* **59** 063514-1 and references therein [SPIRES]
- Damour T and Krauss L M, 1998 *Phys. Rev. Lett.* **81** 5726 [SPIRES]
- [45] Kusenko A and Steinhardt P L, 2001 *Phys. Rev. Lett.* **87** 141301 [SPIRES]
- Gelmini G, Kusenko A and Nussinov S, 2002 *Phys. Rev. Lett.* **89** 101302 [SPIRES]
- [46] Belli P *et al*, 2000 *Phys. Rev. D* **61** 023512 [SPIRES]
- Belli P *et al*, 2002 *Phys. Rev. D* **66** 043503 [SPIRES]
- [47] Savage C, Gondolo P and Freese K, 2004 *Phys. Rev. D* **70** 123513 [SPIRES]
- [48] Gondolo P and Gelmini G, 2005 *Phys. Rev. D* **71** 123520 [SPIRES]
- [49] Bottino A *et al*, 2005 *Phys. Rev. D* **72** 083521 [SPIRES]
- [50] Gunion J F *et al*, 2006 *Phys. Rev. D* **73** 015011 [SPIRES]
- Ferrer F *et al*, 2006 *Phys. Rev. D* **74** 115007 [SPIRES]
- [51] Bird C *et al*, 2004 *Phys. Rev. Lett.* **93** 201803-1 [SPIRES]
- Bird C *et al*, 2006 *Mod. Phys. Lett. A* **21** 457 [SPIRES]
- McDonald J, 1994 *Phys. Rev. D* **50** 3637 [SPIRES]
- Burgess C P *et al*, 2001 *Nucl. Phys. B* **619** 709 [SPIRES]
- [52] Morales A *et al*, 2000 *Phys. Lett. B* **489** 268 [SPIRES]
- Morales A *et al*, 2002 *Astropart. Phys.* **16** 325 [SPIRES]
- [53] Avignone F T *et al*, 1992 *Nucl. Phys. B (Proc. Suppl.)* **28A** 280
- [54] Lee J S and Scopel S, 2007 *Phys. Rev. D* **75** 075001 [SPIRES]
- Scopel S, 2007 private communication
- [55] Dermisek R *et al*, 2007 *Phys. Rev. D* **75** 075019 [SPIRES]
- Dermisek R *et al*, 2006 *Phys. Rev. D* **73** 111701(R) [SPIRES]
- [56] McElrath B, 2007 private communication
- [57] Wong H T and Li H, 2005 *Mod. Phys. Lett. A* **20** 1103 [SPIRES]
- [58] <http://majorana.pnl.gov/>
- [59] <http://www.mpi-hd.mpg.de/ge76/>
- [60] Gonzales D *et al*, 2003 *Nucl. Instrum. Meth. A* **515** 634 [SPIRES]
- Majorovits B and Klapdor-Kleingrothaus H V, 1999 *Eur. Phys. J. A* **6** 463
- [61] Elliot S R *et al*, 2006 *Nucl. Instrum. Meth. A* **558** 504 [SPIRES]
- Abt I *et al*, 2007 Preprint [nucl-ex/0701005](http://arxiv.org/abs/nucl-ex/0701005)